MECHANICS
Vol. 26 No. 2 2007

Peter A. LEWIN*, Andrew W. BERGER**, Christopher J. VECCHIO***, Mark E. SCHAFER****

REMOTE VISUALIZATION OF THE VELOCITY DISTRIBUTION ON VIBRATING STRUCTURES USING THE WAVE FIELD ANALYSIS

SUMMARY

Knowledge of vibrating pattern characteristics is of interest in many applications, including minimization of noise generation in different media and design and optimization of piezoelectric transducers used in diagnostic ultrasound imaging. A field expansion technique developed for analyzing the acoustic fields and vibrating structures is presented. The technique is based on the angular spectrum method of wave-field analysis, and is applicable to both continuous (CW) and wideband pulsed waves, and allows the effects of acoustic parameters such as absorption, dispersion, refraction, and phase distortion to be accounted for. Examples of remotely reconstructed surface velocity distributions of complex acoustic radiators are presented and the potential applications of the technique developed in the analysis of fields radiated by sources with arbitrary geometries, including arrays are also pointed out.

Keywords: *angular spectrum, nonlinear acoustic propagation, acoustic sources*

ZDALNA WIZUALIZACJA ROZKŁADU PRĘDKOŚCI NA DRGAJĄCYCH STRUKTURACH, Z WYKORZYSTANIEM ANALIZY POLA FALI

Wiedza o charakterystyce wzorów drgań znajduje się w obrębie zainteresowania wielu aplikacji, włączając w to minimalizację generacji hałasu w różnych środowiskach oraz projektowanie i optymalizację przetworników piezoelektrycznych używanych do obrazowania w diagnostyce ultradźwiękowej. Zaprezentowano obszar rozwijającej się techniki do analizy pola akustycznego i drgających obiektów. Technika ta bazuje na metodzie spektralnej analizy pola fali za pomocą obciętych szeregów Fouriera i jest stosowana zarówno do ciągłych, jak i szerokopasmowych fal impulsowych, pozwalając na wyliczenie parametrów akustycznych takich, jak pochłanianie, rozpraszanie, załamanie i zniekształcenie fazy. Wyszczególniono również przykłady zdalnie zrekonstruowanych rozkładów pól prędkości złożonych promienników akustycznych oraz potencjalne możliwości zastosowań rozwijanej techniki w analizie pól promieniujących ze źródeł o określonej geometrii; włączając struktury macierzowe.

Słowa kluczowe: *analiza spektralna, nieliniowa propagacja akustyczna, źródło akustyczne*

1. INTRODUCTION

The primary objective of this work was to develop a method that would allow the velocity pattern of vibrating structures to be determined from remote acoustic field measurements. Such method provides an effective tool, particularly useful in the design of ultrasound sources operating in liquid media. In the following sections the theoretical foundations of the technique developed is briefly outlined and experimental verification of the approach in the low megahertz frequency range is presented. Sources of error are identified and the possibilities of further refinement of the model developed are pointed out.

2. THEORY

The model discussed below and used to predict an acoustic field distribution over a plane is based on the angular spectrum method [1–3]. The method has been extended to account for propagation medium (for example, water) nonlinearity. In the angular spectrum approach, acoustic wave propagation between parallel planes is modeled by applying the two-dimensional discrete Fourier transform to samples of a cross-section of an acoustic pressure field. The transform decomposes the grid of samples into a 2-D (two dimensional) spectrum of plane wave components each of which is multiplied by an appropriate phase factor taking into account the propagation distance and the linear characteristics of the propagation media. The resulting propagated spatial spectrum is then inverse transformed to yield a cross-sectional reconstruction of the field at the prediction plane. Each component in the spatial spectrum is multiplied by a corresponding complex propagation term. If $u(x, y, z_0)$ represents an acoustic particle velocity field distribution over a plane parallel to the (x, y) plane and passing through the point z_0, then let $U(\omega_x, \omega_y, z_0)$ be the 2-D Fourier transform of this function. The Fourier transform decomposes the field contour into a 2-D spectrum in which the magnitude and phase at each spatial frequency (ω_x, ω_y) represent the magnitude and phase of a plane wave travelling with unique direction cosines ($n_x = \omega_x/k$, $n_y = \omega_y/k$), where k is the wavenumber in the medium. Propagation may be modeled by

* School of Biomedical Engineering and Electrical and Computer Engineering, Drexel University Philadelphia, PA 19104, USA; lewin@ece.drexel.edu
** Dept. of Physics & Electrical Engineering, University of Scranton, PA 18510
*** Spectrasonics, Inc., Wayne, PA 19087
**** Sonic Technologies, Ambler, PA 19002

multiplying each (ω_x, ω_y) frequency component by a phase propagation factor to account for plane wave travel in the (n_x, n_y) direction. The phase change can be expressed as [1, 4]

$$G(\omega_x, \omega_y, z_1 - z_o) = \\ = \exp\left[-j(z_1 - z_o)(k^2 - \omega_x^2 - \omega_y^2)^{1/2}\right] \equiv \\ \equiv e^{\phi(\omega_x, \omega_y, z_1 - z_o)} \quad (1)$$

Equation (1) specifies the way in which the elements in the phase propagation array are determined. $G(\omega_x, \omega_y, z_1–z_0)$ is a factor, which introduces the phase change $\phi(\omega_x, \omega_y, z_1–z_0)$ to account for the propagation from the plane at z_0 to the plane at z_1. Thus, if each (ω_x, ω_y) term in the angular spectrum of the field at z_0 is multiplied by the appropriate phase factor $G(\omega_x, \omega_y, z_1–z_0)$, the complex pressure field at z_1 can be found by inverse Fourier transforming the resultant (propagated) two-dimensional spectrum of components. This can be stated as follows

$$u(x, y, z_1) = \\ = \frac{1}{\sqrt{2\pi}} \int_{-\infty}^{\infty} \int U(\omega_x, \omega_y, z_o) e^{\phi(\omega_x, \omega_y, z_1 - z_o)} e^{j(\omega_x X + \omega_y Y)} d\omega_x d\omega_y \quad (2)$$

Equation (2) demonstrates the way in which the pressure field across a plane at z_1, $u(x, y, z_1)$, can be found from the Fourier transform of the field at z_0, $U(\omega_x, \omega_y, z_0)$, and the phase factor, $e^{\phi(\omega_x, \omega_y, z_1 - z_0)}$. Note that if the quantity $(\omega_x^2+\omega_y^2)$ is less than k^2 in equation (1), the exponent in the phase factor will be purely imaginary and will introduce the phase changes undergone during propagation from z_0 to z_1. When $(\omega_x^2+\omega_y^2)$ is greater than k^2, the exponent in $G(\omega_x, \omega_y, z_1–z_0)$ becomes negative and real. Waves propagating at these spatial frequencies decay exponentially with distance and are known as evanescent waves. Because they are rapidly attenuated, evanescent components do not present any computational difficulties in the forward propagation case.

Implicit in the linear form of the angular spectrum model is an assumption that the sound speed in any medium is constant and does not vary with changes in acoustic pressure. This assumption of linear behavior is inaccurate for propagation through many media such as water or tissue, particularly when high acoustic pressure amplitudes are used [5–7]. For this reason, to accurately model the propagation of acoustic waves, it is desirable to account for the effects due to the nonlinear nature of the investigated medium [19]. The theoretical basis of the technique used for modeling such nonlinear propagation phenomena can be found in [8–15]. For a plane wave traveling in the $+z$ direction, the incremental change in particle velocity U for the n^{th} harmonic is given by

$$U_n(z + \Delta z) = \\ = U_n(z) - \frac{i\beta\omega_o}{c_o^2}\left\{\sum_{k=1}^{n-1} kU_k U_{n-k} + \sum_{k=n}^{\infty} nU_k U_{k-n}^*\right\}\Delta z \quad (3)$$

In the above equation (3) c_0 is the infinitesimal bulk acoustic wave velocity (dispersion is neglected), $\beta = \left(1 + \frac{B}{2A}\right)$, where B/A is the first term in the thermodynamic pressure-density relation [16], and ω_0 is the fundamental frequency of the wave.

Equation (3) describes the spectral changes which occur in an acoustic plane wave due to nonlinear propagation over an incremental distance Δz. For a multi-harmonic plane wave traveling in the $+z$ direction, the difference $U_n(z) – U_n(z+ \Delta z)$ describes the incremental change in particle velocity U for the n^{th} harmonic. As an acoustic wave propagates through a nonlinear medium additional frequencies are generated. As in a nonlinear mixing operation, the (sum and difference) frequencies produced are harmonically related to those present in the initial spectrum. There are two summations within the large brackets of equation (3) and these represent the generation and depletion of harmonics as the wave propagates over the incremental distance, Δz. Contributing to the n^{th} harmonic frequency are all the harmonic pairs whose sum or difference is n. Equation (3) was used to extend the angular spectrum model to include the effects of nonlinear phenomena on acoustic propagation.

3. EXPERIMENTAL METHODS

A block diagram of the experimental system is shown in Figure 1. Pressure waveforms produced by acoustic sources were sampled by pre-amplified 0.3 mm diameter PDVF needle-type hydrophones (SEA model PVDFZ4, CA USA, and Force Institute, Copenhagen). The frequency response of the probe was determined to be within +/– 1 dB over the ranges of 1–30 MHz and 1–20 MHz, respectively [17]. The maximum peak pressures encountered in the experiments were on the order of several MPa. Once acquired, basis datasets were processed by the system to yield predictions of the field contours at other cross-sectional planes. Cross-sectional measurements were also made at certain distances for purposes of comparison with predictions.

A typical dataset was composed of a 128×128 point raster scan of spatial datapoints. Each datapoint required approximately 1 second to acquire and therefore the acquisition of a complete dataset required approximately 8 hours. Particle velocity fields were calculated from the measured pressure fields using the impedance relation [20], $u = (p/\rho_0 c_0)$. Dedicated PC was used to control both the positioning of the hydrophone probe and the collection of data which was digitized by a Tektronix 2440 oscilloscope.

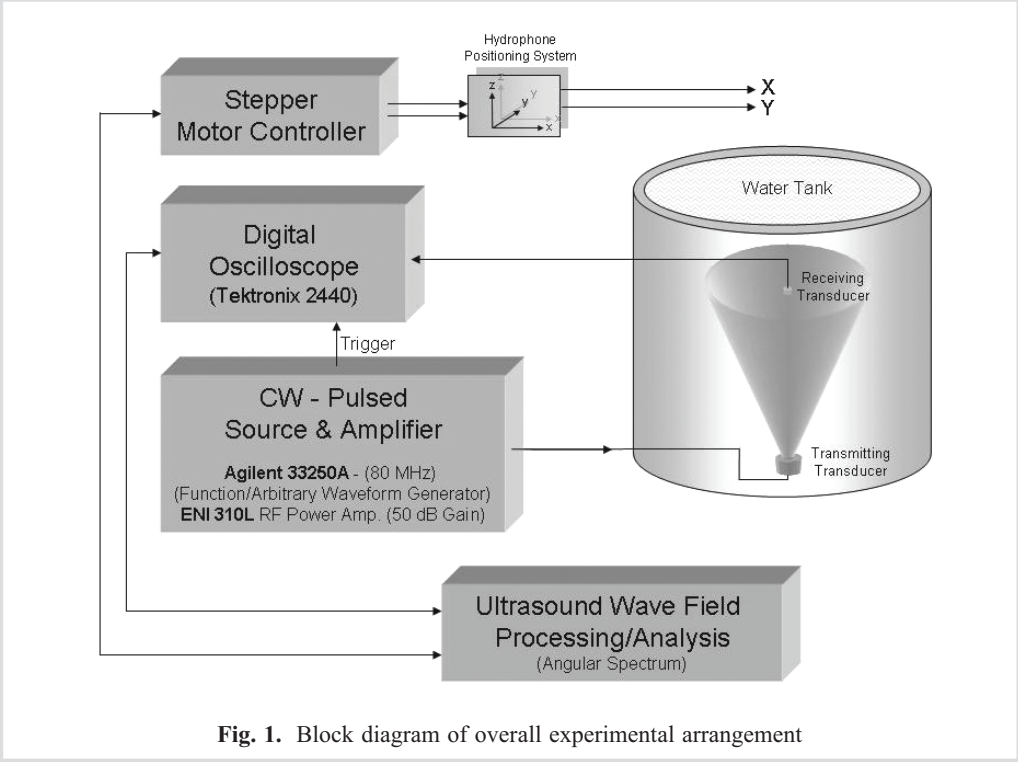

Fig. 1. Block diagram of overall experimental arrangement

4. RESULTS

Several experiments were conducted to test the nonlinear angular spectrum model. To provide initial validation, the model was applied to simulated source distributions and the results compared with those obtained using independent models [15, 18, 19]. Subsequently, the model was applied to experimental data and the results compared with measurements. Experiments were designed to test the system's ability to predict linear acoustic propagation in both the forward and backward cases and nonlinear propagation in the forward case. Experiments were also designed to demonstrate the model's applicability to complex transducer geometries and pulsed (versus CW) excitation. Selected results of the simulations and experiments are presented below. Except where noted, the three dimensional contour graphs display the magnitude of the fundamental frequency component of the particle velocity field.

All tests were conducted at room temperature (25°C). The frequency dependent attenuation [20] and nonlinearity (B/A) [21] parameters in the medium (water) were assumed to be $2.5\cdot10^{-14}\ \mathrm{Np}\cdot\mathrm{s}^2/m$ ($\alpha = 2.5\cdot10^{-14}\cdot f^2$) and 5.0, respectively. In Figure 2a the results corresponding to a half-moon, 3 MHz, 18 mm focused source are shown. Such sources are used in CW Doppler systems to detect liquid movement or heart motion and measure blood flow in the human body. Figure 2a shows measured particle velocity amplitude at 5 mm axial distance, whereas in Figure 2b predicted phase of the transducer surface velocity profile is displayed. In another experiment a circular, 3 MHz focused source was exited by a monocycle tone burst. A small brass rod was glued in the center of this 7 mm diameter transducer to test the ability of the angular spectrum method to identify variations in the source vibrating pattern (see Fig. 3).

In Figure 3a the distribution of the particle velocity magnitude measured at the axial distance of 10 mm is displayed. Figure 3b shows the phase of the reconstructed surface velocity.

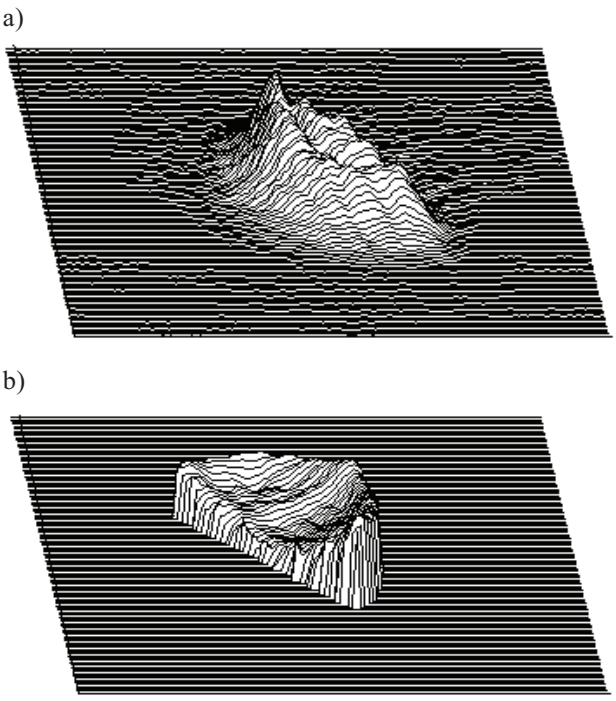

Fig. 2. Measured particle velocity magnitude 5.0 mm in front of a 3.0 MHz, semi-circular, focused source used as a basis for predictions (a); phase of the transducer surface velocity profile predicted from 5.0 mm measurement (b). After [12–14]

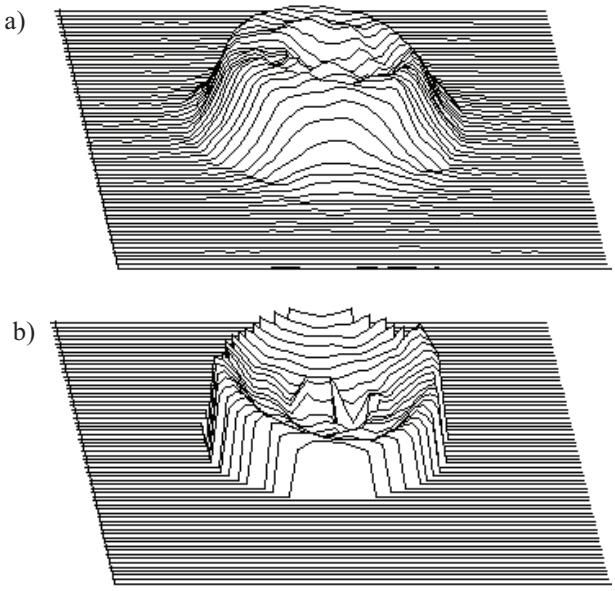

Fig. 3. Magnitude of the transducer surface velocity profile predicted from 10.0 mm measurement (a); phase of the transducer surface velocity profile predicted from 10.0 mm measurement (b). After [12–14]

The predicted particle velocity amplitudes of the fundamental and second harmonic components as functions of distance along the measurement axis are shown in Figure 4a along with the experimentally measured axial amplitudes. Plots of the measured and predicted higher harmonics amplitudes (second and third) are shown in Figure 4b.

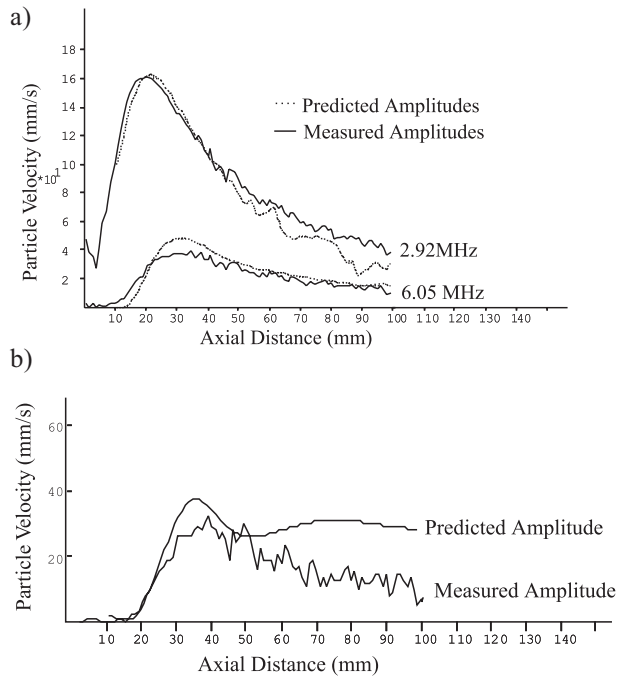

Fig. 4. Measured and predicted fundamental and second harmonic pressure amplitudes as functions of axial distance for a 3.0 MHz, 7.0mm diameter, focused source (a); measured and predicted third harmonic pressure amplitudes as functions of axial distance for a 3.0 MHz, 7.0mm diameter, focused source (b). After [12–14]

5. DISCUSSION

In Figures 2 and 3 the results of applying the model to the field produced by a complex, non-axially symmetric source geometry are presented. The source examined was 18.0 mm in diameter, focused, and semi-circular in shape. In both backward propagated images of the surface particle velocity (Fig. 2b) the semi-circular shape of the acoustic source can be clearly identified. Examination of the phase image also reveals the surface curvature of the focused source. The phase image is tilted slightly indicating that the source was not aligned precisely perpendicular to the measurement plane. The predicted phase image of the surface particle velocity of the focused, 7.0 mm diameter transducer is shown in Figure 3b. As in the image of the semi-circular transducer of Figure 2, examination of the phase plot reveals both the outline and the surface curvature of the focused source. A discontinuity in the center of the surface velocity profile due to the glued small brass rod can also be seen. Predicted and measured axial amplitudes for this transducer are shown in Figures 4a and 4b, respectively. The measured and predicted fundamental and second harmonic particle velocity amplitudes correlate closely. There are significant discrepancies between the measured and predicted third harmonic amplitudes, however. These discrepancies are due to the limited number of harmonics included in the model. Because of the sampling requirements of pulsed operation, the fundamental frequency of the source fell between the fourth and fifth frequency bins in this experiment. Therefore, even though 64 frequency bins were used, only four harmonics of the nominal 3.0 MHz fundamental were present in the analysis. As the propagating field became increasingly shocked, the energy which should have been transferred into upper harmonics, accumulated in the limited number of high frequencies present in the model. Because of this, error which increases with distance is present in the third harmonic prediction. The measured and predicted field particle velocity magnitudes on the acoustic axis are within 1.0 dB.

6. CONCLUSIONS

The results obtained in this work demonstrate the applicability of the extended angular spectrum approach to the analysis of acoustic field propagation through nonlinear liquid media. The backward propagated images presented reaffirm the value of the technique in the examination and visualization of the vibrating structure behavior. Even in situations in which the field contours were significantly diffracted, the method was able to provide detailed surface velocity contour reconstructions. Comparisons between measured field contours, linear, and nonlinear predictions have shown the importance of including nonlinear phenomena when modeling acoustic propagation. Additionally, the angular spectrum model's applicability to cases in which acoustic fields are produced by a complex, non-axially symmetric radiators has been verified.

The method holds particular promise for use as a tool in the design and optimization of acoustic radiators. The ulti-

mate goal of this research is to develop the model to the point where it will provide information on the degradation of ultrasonic transducer performance due to propagation through complex nonlinear media such as biological tissue.

References

[1] Stepanishen P.R., Benjamin K.C.: *Forward and backward projection of acoustic fields using FFT methods.* J. Acoust. Soc. Am., 71, 1982, 803–811

[2] Schafer M.E., Lewin P.A.: *Transducer characterization using the angular spectrum Method.* J. Acoust. Soc. Am., 85 (5), 1989, 2202–2214

[3] Goodman J.W.: *Introduction to Fourier Optics.* New York, McGraw--Hill 1968

[4] Higgins F.P., Norton S.J., Linzer M.: *Optical interferometric visualization and computerized reconstruction of ultrasonic fields.* J. Acoust. Soc. Am., 68, 1980, 1169–1176

[5] Starritt H.C., Perkins M.A., Duck F.A., Humphrey V.F.: *Evidence for ultrasonic finite-amplitude distortion in muscle using medical equipment.* J. Acoust. Soc. Am., 77 (1), 1985, 302–306

[6] Bacon D.R., Carstensen E.L.: *Increased Heating by diagnostic ultrasound due to nonlinear propagation.* J. Acoust. Soc. Am., 88 (1), 1990, 26–34

[7] Zeqiri B.: *Errors in attenuation measurements due to nonlinear propagation effects.* J. Acoust. Soc. Am., 91 (5), 1992, 2585–2593

[8] Blackstock D.T.: *Thermoviscous Attenuation of Plane, Periodic, Finite Amplitude Sound Waves.* J. Acoust. Soc. Am., 36, 1964, 534–542

[9] Korpel A.: *Frequency approach to nonlinear dispersive waves.* J. Acoust. Soc. Am., 67 (6), 1980, 1954–1958

[10] Trivett D.H., Van Buren A.L.: *Propagation of plane, cylindrical, and spherical finite amplitude waves.* J. Acoust. Soc. Am., 69 (4), 1981, 943–949

[11] Haran M.E., Cook B.D.: *Distortion of Finite Amplitude Ultrasound in Lossy Media.* J. Acoust. Soc. Am., 73, 1983, 774–779

[12] Vecchio C.J.: *Finite amplitude acoustic propagation modeling using the extended angular spectrum method.* Ph.D. Thesis, Drexel University, 1992

[13] Vecchio C.J., Lewin P.A.: *Finite amplitude propagation modeling using the extended angular spectrum method.* J. Acoust. Soc. Am., 95 (5), 1994, 2399–2408

[14] Vecchio C.J., Lewin P.A.: *Prediction of ultrasonic field propagation through layered media using the extended angular spectrum method.* Ultrasound in Medicine and Biology, vol. 20 (7), 1994, 611–622

[15] Radulescu E.G., Wojcik J., Lewin P.A., Nowicki A.: *Nonlinear Propagation model for ultrasound hydrophones calibration in the frequency range up to 100 MHz.* Ultrasonics, 41, 2003, 231–245

[16] Beyer R.T.: *Nonlinear Acoustics.* US G.P.O, Washington, D.C., 1977, 95–109

[17] Lewin P.A.: *Miniature piezoelectric polymer ultrasonic hydrophone probes.* Ultrasonics, 19, 1981, 213–216

[18] Baker A.C.: *Nonlinear pressure field due to focused circular apertures.* J. Acoust. Soc. Am., 91, 1992, 713–717

[19] Christopher P.T., Parker K.J.: *New approaches to nonlinear diffractive field Propagation.* J. Acoust. Soc. Am., 90, 1991, 488–499

[20] Kinsler L.E., Frey A.R.: *Fundamentals of Acoustics.* Third Edition, (John Wiley &Sons, New York), 1982, 110–152

[21] Muir T.G., Cartensen E.L.: *Demonstration of nonlinear acoustic effects at biomedical frequencies and intensities.* Utrasound in Medicine and Biology, vol. 6, 1980, 359–368